Cyclooxygenase production of PGE_2 promotes phagocyte control of *A. fumigatus* hyphal growth in larval zebrafish

Savini Thrikawala[1], Mengyao Niu[2], Nancy P. Keller[2,3], Emily E. Rosowski[1*]

[1]Department of Biological Sciences, Clemson University, Clemson, South Carolina, United States of America

[2]Department of Medical Microbiology and Immunology, University of Wisconsin-Madison, Madison, Wisconsin, United States of America

[3]Department of Bacteriology, University of Wisconsin-Madison, Madison, Wisconsin, United States of America

* Corresponding author

E-mail: erosows@clemson.edu

Abstract

Invasive aspergillosis is a common opportunistic infection, causing >50% mortality in infected immunocompromised patients. The specific molecular mechanisms of the innate immune system that prevent pathogenesis of invasive aspergillosis in immunocompetent individuals are not fully understood. Here, we used a zebrafish larva-*Aspergillus* infection model to identify cyclooxygenase (COX) enzyme signaling as one mechanism that promotes host survival. Larvae exposed to the pan-COX inhibitor indomethacin succumb to infection at a significantly higher rate than control larvae. COX signaling is both macrophage- and neutrophil-mediated. However, indomethacin treatment has no effect on phagocyte recruitment. Instead, COX signaling promotes phagocyte-mediated inhibition of germination and invasive hyphal growth. Protective COX-mediated signaling requires the receptor EP2 and exogenous prostaglandin E_2 (PGE_2) rescues indomethacin-induced decreased immune control of fungal growth. Collectively, we find that COX signaling activates the PGE_2-EP2 pathway to increase control *A. fumigatus* hyphal growth by phagocytes in zebrafish larvae.

Author Summary

Invasive aspergillosis causes mortality in >50% of infected patients. It is caused by a free-living fungus *Aspergillus fumigatus* which releases thousands of airborne spores. While healthy individuals clear inhaled spores efficiently, in immunocompromised individuals these spores grow into filamentous hyphae and destroy lungs and other tissues causing invasive aspergillosis. The immune mechanisms that control this fungal growth in healthy people are still largely unknown. Here, we used a larval zebrafish model of *A. fumigatus* infection to determine that cyclooxygenase enzymes, which are the target of non-steroidal anti-inflammatory drugs such as

aspirin and ibuprofen, are important to control the fungus. Innate immune cells use cyclooxygenase signaling to prevent hyphal growth and tissue destruction. Our study provides new insights into the mechanisms that immune cells deploy to stop invasive growth of *A. fumigatus* and inform development of future strategies to combat invasive aspergillosis.

Introduction

Aspergillus fumigatus is a free-living saprophytic fungus which reproduces asexually by producing thousands of conidia or spores. Owing to their small size and hydrophobicity, spores become airborne causing widespread contamination both indoors and outdoors. It is estimated that an average person can inhale 100-1000 spores per day (1). Although healthy immune systems can combat these spores, in immunocompromised individuals spores can germinate to form invasive hyphae which spread to multiple organs and tissues—a condition called invasive aspergillosis (IA) (1). IA remains a major cause of mortality in immunocompromised patients, particularly individuals with hematological malignancies, bone marrow or solid-organ transplant recipients, HIV patients, ICU patients, and patients with altered lung conditions (2). Despite the availability of anti-fungal drugs, the mortality rate of IA remains at ~50% (3-5). Hence, it is imperative to develop novel strategies to target fungi and augment anti-fungal immune responses, but this requires a better understanding of immune cell-pathogen interactions. Innate immune cells act as the first line of defense against inhaled *A. fumigatus* conidia. However, the signaling and effector mechanisms that these cells use to inhibit fungal growth are not fully understood.

Eicosanoids, such as prostaglandins, are arachidonic acid-derived lipid signaling molecules that function in both an autocrine and paracrine manner by binding to their receptors and can have a

variety of effects on immune cell function (6, 7). Prostaglandins are produced by prostaglandin endoperoxide H synthases (PGHSs), also called cyclooxygenase (COX) enzymes. COX enzymes are the target of non-steroidal anti-inflammatory drugs such as aspirin, ibuprofen and indomethacin (8-10). COX-derived prostaglandins can have either pro- or anti-inflammatory effects on innate immune cells, modulating both phagocyte recruitment and phagocyte functions (6, 7, 11). In response to fungal pathogens, prostaglandin signaling is known to inhibit phagocytosis of *Candida albicans* by macrophages, H_2O_2-mediated fungicidal activity against *Paracoccidioides brasiliensis*, and M1 polarization of alveolar macrophages and killing of *Cryptococcus neoformans* (12-14). However, the roles of COX activation and prostaglandins during *A. fumigatus* infections are not known.

Analyzing how given pathways affect specific aspects of dynamic host-pathogen interactions *in vivo* is challenging. The zebrafish larva-*Aspergillus* infection model overcomes many of these challenges, as larvae are transparent and allow for direct visualization of phagocyte-*Aspergillus* interactions through high-resolution repetitive imaging of the same larvae over the course of a multi-day infection (15). Multiple steps in pathogenesis such as phagocyte recruitment, phagocytosis, spore killing, germination, and hyphal growth or clearance can be quantified using this live imaging technique (16). Zebrafish have a well-conserved immune system with humans, but depend solely on their innate immune system for the first few weeks of their life, providing a window to study innate immune mechanisms with no interference from the adaptive system (17, 18). The zebrafish larva-*Aspergillus* model recapitulates multiple aspects of human IA: while immunocompetent larvae are resistant, immunocompromised larvae are susceptible to the infection and develop invasive hyphae (19, 20).

Here we use this zebrafish larva-*Aspergillus* infection model to determine the role of the host COX pathway in phagocyte-mediated *A. fumigatus* clearance. We find inhibition of host COX signaling increases spore germination and invasive growth of hyphae in infected larvae, thereby decreasing host survival. COX signaling does not affect macrophage or neutrophil recruitment but instead activates these cells to target the fungus. Exogenous PGE_2 injection restores control of hyphae in COX-inhibited larvae, suggesting that PGE_2 is a major driver of COX-mediated control of fungal growth by phagocytes.

Results

Host cyclooxygenase inhibition decreases infected larval survival

Prostaglandins are lipid signaling molecules whose production is induced during inflammation via cyclooxygenase (COX) enzymes. We used the zebrafish larva-*Aspergillus* infection model to test the hypothesis that host COX signaling promotes larval survival and fungal clearance in an *A. fumigatus* infection. Wild-type *A. fumigatus* spores were microinjected into the hindbrain ventricle of 2 days post fertilization (dpf) larvae. Infected larvae were then exposed to the pan-COX inhibitor indomethacin or DMSO vehicle control immediately after injection and larval survival was monitored for 7 days. Indomethacin is a well-established non-steroidal anti-inflammatory drug that inhibits COX enzyme activation and prostaglandin synthesis (9, 10) and is widely used in a variety of animal models including zebrafish (21, 22). Indomethacin-treated larvae succumb to infection at a significantly greater rate than control larvae (Fig 1A). Treatment with the COX1 inhibitor SC560 (23) or COX2 inhibitor meloxicam (21) also significantly

114 increases infected larval mortality (S1 Fig). With each of these inhibitors, no significant decrease
115 in survival was observed in mock-infected larvae (Fig 1A and S1 Fig).
116
117 *A. fumigatus* also harbors three Ppo enzymes (PpoA, PpoB and PpoC) with high identity to
118 vertebrate COX (24), but a previous study reported that indomethacin does not affect the
119 function of these enzymes (25). To confirm that the observed effects of indomethacin on infected
120 larval survival are not due to inhibition of fungal enzymes, we infected zebrafish larvae with *A.*
121 *fumigatus* spores lacking all three *ppo* genes (Δ*ppoA*, Δ*ppoB*, Δ*ppoC*) (S2 Fig). Deletion of *ppo*
122 enzymes had no effect on fungal virulence, as survival of larvae infected with triple-*ppo*-mutant
123 *A. fumigatus* spores is similar to larvae infected with wild-type spores (Fig 1B). Additionally,
124 indomethacin treatment decreased survival equally in larvae infected with triple-*ppo*-mutant and
125 wild-type spores (Fig 1B). These data demonstrate that indomethacin inhibits host enzymes to
126 compromise survival of *A. fumigatus*-infected larvae. Since no survival difference was observed
127 in larvae infected with a triple-*ppo*-mutant, we focused on wild-type *A. fumigatus* for the
128 remainder of the study.
129
130 Among COX-biosynthesized prostaglandins, prostaglandin E_2 (PGE_2) is a major product
131 synthesized by phagocytes that moderates a range of inflammatory processes and has pro- or
132 anti-inflammatory functions, depending on the receptor to which it binds (26). PGE_2 elicits its
133 actions via four different E type prostanoid receptors, EP1-4, with most immunomodulatory
134 effects mediated via EP2 and EP4 (26). Therefore, we tested if EP2 and 4 receptor antagonists
135 affect the disease outcome of *A. fumigatus*-infected larvae. We used antagonists of EP2: AH6809
136 (27) and EP4: AH23848 (22, 27, 28) previously used in zebrafish larvae. Larvae exposed to

AH6809 succumb to the infection at a similar rate as indomethacin-exposed larvae, both with a hazard ratio of 3 compared to control larvae, while AH23848-exposed larvae show no significant difference in survival compared to control (Fig 1C). These data suggest that COX signaling promotes *A. fumigatus*-infected larvae survival via a PGE_2-EP2 signaling pathway.

Both macrophages and neutrophils use cyclooxygenase signaling to combat *A. fumigatus* infection

We next sought to determine which innate immune cells utilize COX signaling to fight *A. fumigatus* infection. Macrophages and neutrophils are the primary immune cells that combat *A. fumigatus* infection in zebrafish larvae (20). To determine if these cell types play a role in COX-mediated host responses, we inhibited development of both phagocytes by knocking down *pu.1 (spi1b)* via morpholino injection (29). If COX signaling activates phagocytes to clear the infection, we expect that indomethacin treatment of larvae that are already depleted of phagocytes would have no effect on larval survival. Larvae were injected with *A. fumigatus* spores or PBS and exposed to indomethacin or DMSO. Indomethacin exposure significantly decreases survival of larvae injected with a control morpholino but has no effect on *pu.1* morphants (Fig 2A, S3A Fig), suggesting that COX-mediated host protection is phagocyte-dependent.

Then we interfered with macrophage and neutrophil function individually to determine if each cell type is required for COX-mediated host protection. We injected 1 dpf larvae with clodronate liposomes to deplete macrophages or PBS liposomes as a control. As observed previously,

160 macrophage-depleted larvae rapidly succumb to the infection (20). However, indomethacin
161 exposure further decreases the survival of macrophage-depleted larvae (Fig 2B). While
162 indomethacin treatment makes control larvae 8.4 times more likely to succumb to infection,
163 clodronate liposome-injected larvae are only 1.7 times more likely to succumb upon
164 indomethacin treatment (Fig 2B), suggesting that macrophages partially mediate the host-
165 protective effects of COX signaling, but that even in the absence of macrophages COX signaling
166 increases host survival. Larvae injected with clodronate liposomes and then given a PBS mock
167 infection also have lower survival upon indomethacin treatment, suggesting that some of this
168 death may be due to the effects of the clodronate alone, although this difference in PBS mock-
169 infected larvae is not statistically significant (S3B Fig).
170
171 We next tested the survival of neutrophil-defective (*mpx:rac2D57N*) infected larvae. In these
172 larvae neutrophils are unable to migrate to the infection site (30). As found previously,
173 neutrophil-defective larvae are more susceptible to *A. fumigatus* infection than wild-type controls
174 (Fig 2C) (20, 31). Indomethacin exposure further decreases survival of neutrophil-defective
175 larvae (Fig 2C). Compared to wild-type larvae which are 3.9 times more likely to succumb to
176 infection, neutrophil-defective larvae are only 1.8 times more likely to succumb to infection,
177 suggesting that neutrophils also partially mediate the host-protective effects of COX signaling,
178 but that other cell types can be involved. Lack of neutrophils has no effect on survival of mock-
179 infected larvae treated with indomethacin (S3C Fig). Together, these data demonstrate that both
180 macrophages and neutrophils participate in COX-mediated responses to promote survival of *A.*
181 *fumigatus*-infected zebrafish larvae.
182

Cyclooxygenase activity is not required for phagocyte recruitment

We next sought to define how the innate immune response is altered by COX inhibition. COX-synthesized prostaglandins are chemical messengers that can function to recruit immune cells to infection sites, and we wondered whether COX inhibition affects macrophage or neutrophil recruitment to *A. fumigatus* infection (7, 20). Zebrafish larvae expressing GFP in macrophages (*Tg(mpeg1:H2B-GFP)*) or BFP in neutrophils (*Tg(lyz:BFP)*) were infected with *A. fumigatus* spores expressing mCherry, and treated with indomethacin or DMSO vehicle control and we enumerated the number of macrophages and neutrophils at the infection site through daily confocal imaging (Fig 3A).

As described previously, macrophages are recruited starting at 1 day post infection (dpi) and form clusters around spores starting at 2-3 dpi (Fig 3B), with neutrophils primarily responding after spores germinate (Fig 3C). The number of recruited macrophages (Fig 3D), macrophage cluster area (Fig 3E), and the number of recruited neutrophils (Fig 3F) are not significantly different between indomethacin- and DMSO-exposed groups at days 1, 2, and 3 post infection. At 5 dpi, however, more macrophages (Fig 3D) and neutrophils (Fig 3F) are found at the infection site in indomethacin-treated larvae. Fungal germination occurs at these later time stages and attracts more immune cells. To control for this variable, we analyzed the number of macrophages and neutrophils in each larva relative to the day germination and invasive hyphae were first observed. Using this normalization, we find that macrophage numbers (Fig 3G) and neutrophil numbers (Fig 3H) are similar between the two conditions at each stage of fungal pathogenesis. Overall, our results indicate that phagocyte recruitment is not dependent on COX activation.

Cyclooxygenase activity does not promote spore killing

We next hypothesized that the functions of these phagocytes are modulated by COX signaling. The initial response of macrophages is to phagocytose injected spores and activate spore killing mechanisms (19, 20). To determine if COX inhibition affects spore killing, we used a live-dead staining method in which *A. fumigatus* spores expressing YFP are coated with AlexaFluor 546 and injected into zebrafish larvae expressing mTurquoise in macrophages (20, 32). Larvae were imaged with confocal microscopy at 2 dpi, and we enumerated the number of live versus dead spores. Live spores are visualized as YFP signal surrounded by AlexaFluor signal, while dead spores only have AlexaFluor signal (Fig 4A). The percentage of live spores is similar in indomethacin and DMSO groups both within macrophages and in the whole imaged hindbrain area (Fig 4B). To confirm these results, we also measured the overall fungal burden in indomethacin- or DMSO-treated larvae over the 7-day infection period with CFU counts. Consistent with live-dead staining, the fungal burden is similar between DMSO- and indomethacin-exposed larvae throughout the infection (Fig 4C), indicating that COX signaling does not drive spore clearance.

Cyclooxygenase inhibition decreases immune control of fungal germination

As spore killing is not affected by COX inhibition, we next hypothesized that immune control of the next stages in fungal pathogenesis—spore germination and invasive hyphal growth—is modulated by COX signaling. To monitor spore germination and hyphal growth in larvae, we infected larvae with *A. fumigatus* spores expressing mCherry and imaged at 1, 2, 3 and 5 dpi with

confocal microscopy. We find spore germination in both indomethacin- and DMSO-exposed larvae (Fig 5A). However, both the rate at which larvae are observed to have germination inside of them and the total percentage of larvae that harbor germinated spores is significantly higher in the presence of indomethacin (Fig 5B).

Since germination is increased upon indomethacin treatment, we wanted to confirm again that the effects of indomethacin are on the host and that indomethacin does not directly alter *A. fumigatus* germination. To test this, *A. fumigatus* spores were inoculated *in vitro* in liquid RPMI medium in the presence of indomethacin or DMSO and the percentage of germinated spores was scored at 2-hour intervals. We find no difference in the rate of germination between indomethacin and DMSO-treated spores (S4 Fig). Therefore, our data demonstrate that indomethacin decreases host immune cell-mediated control of *A. fumigatus* germination.

Cyclooxygenase inhibition decreases immune control of invasive hyphal growth

After germination, *A. fumigatus* hyphae branch and grow into a network disrupting the host tissue. The cumulative percentage of larvae with invasive hyphae (as defined by branched hyphal growth (S5 Fig)) is also significantly higher with indomethacin treatment (Fig 5B). We also quantified the hyphal burden by measuring the fungal area, finding more extensive hyphal growth in indomethacin-treated larvae at both 3 and 5 dpi, although this difference is not statistically significantly (Fig 5C), likely due to high variability between larvae and the large number of indomethacin-treated larvae that succumbed to infection before 5 dpi (Fig 1A). Next, we rated the severity of fungal growth on a scale of 0 to 4, from no germination to severe

invasive growth of hyphae, and a lethal score of 5 (S5 Fig). Severe growth of invasive hyphae is prominent in larvae exposed to indomethacin, eventually causing mortality (Fig 5D). Although germination occurred in the vehicle control group, these larvae are able to delay invasive growth compared to indomethacin-treated larvae (Fig 5D), suggesting that the major defect in these larvae is a failure to control hyphal growth post-germination. To quantify this time of delay between appearance of germination and invasive hyphae, we analyzed the timeline of first appearance of germlings and invasive hyphae in larvae more closely, focusing only on larvae that had germination within them at some point in the experiment. We quantified the day germination was first observed, the day invasive hyphae was first observed, and the time between these two occurrences. The day to first observe germination was similar between the two groups (Fig 5E). However, invasive hyphae appear significantly earlier after both initial infection (Fig 5F) and after germination (Fig 5G) in indomethacin-exposed larvae. Once spores are germinated, invasive hyphae appear on average ~1 day later in control larvae, while in indomethacin-treated larvae, this growth only takes an average of ~0.5 days (Fig 5G). Together, these results suggest that COX signaling promotes phagocyte-mediated control of invasive hyphal growth.

Neutrophils are thought to be the major phagocyte that targets and kills invasive hyphae. In *irf8*$^{-/-}$ larvae which lack macrophages and have an abundance of neutrophils, neutrophils destroy fast-germinating strains of *A. fumigatus* such as CEA10 within a few days (20). We therefore decided to use this infection scenario to specifically test the requirement for COX signaling in neutrophil-mediated hyphal killing. We infected *irf8*$^{-/-}$ larvae with CEA10 spores and isolated larvae for CFU enumeration at 0, 1, and 2 dpi. CFUs from *irf8*$^{-/-}$ were normalized to CFUs of *irf8*$^{+/+}$/*irf8*$^{+/-}$

at each dpi for each condition. At 2 dpi in DMSO-treated larvae, ~26% of the fungal burden remains in *irf8*$^{-/-}$ larvae compared to macrophage-sufficient larvae (*irf8*$^{+/+}$ or *irf8*$^{+/-}$), demonstrating the neutrophil-mediated clearance of fungus that occurs in these larvae (S6A Fig). Fungal clearance is slightly alleviated but not significantly different in indomethacin-exposed *irf8*$^{-/-}$ larvae, suggesting that COX signaling may promote but is not required for neutrophil-mediated killing of hyphae (S6A Fig). Similar to infection with Af293-derived strains, CEA10-infected larvae also succumb to the infection at a higher rate in the presence of indomethacin both in *irf8*$^{+/+}$/*irf8*$^{+/-}$ and *irf8*$^{-/-}$ backgrounds (S6B Fig).

Exogenous PGE_2 increases immune control of hyphal growth in the presence of indomethacin

So far we have established that COX signaling promotes macrophage- and neutrophil-mediated control of germination and invasive hyphal growth in an *A. fumigatus* infection. It is likely that COX signaling acts via a PGE_2-EP2 signaling axis, as EP2 receptor antagonist-treated infected larvae succumb to infection at the same rate as indomethacin-treated larvae (Fig. 1C). We therefore tested if exogenous PGE_2 can rescue the effects of indomethacin treatment in infected larvae. Since PGE_2 is short-lived and elicits short-range effects, we injected *A. fumigatus*-infected, indomethacin- or DMSO-treated larvae with PGE_2 or DMSO vehicle control into the hindbrain at 1 dpi. PGE_2 injection partially rescues survival of indomethacin-treated larvae, although the effect is not statistically significant (Fig 6A). To determine if PGE_2 can rescue indomethacin-inhibited functions of phagocytes against invasive fungal growth, we imaged the larvae at 3 dpi. As seen previously, indomethacin treatment increases the percentage of larvae

harboring both germination and invasive hyphae at 3 dpi (Fig 6B). Quantification of 2D fungal area further supports this observation (Figs 6C, D). PGE_2 supplementation rescues these phenotypes, decreasing germination, development of invasive hyphae, and total fungal burden (Figs 6B-D), without affecting phagocyte recruitment (S7A and S7B Figs). However, in the absence of indomethacin treatment, exogenous PGE_2 actually leads to increased fungal germination and invasive hyphae (Fig 6B). Additional experiments also demonstrate that PGE_2 injection does not increase survival of either wild-type or neutrophil-defective larvae not treated with indomethacin (Fig 6A, S7C Fig). These data suggest that the level of PGE_2 during infection must be strictly controlled as too much PGE_2 is also detrimental to control of *A. fumigatus*. Collectively, our findings demonstrate that COX-mediated PGE_2 production and signaling via the EP2 receptor promotes phagocyte-mediated control of *A. fumigatus* germination and hyphal growth (Fig 7).

Discussion

Healthy immune systems can contain and kill *A. fumigatus* spores despite the fact that hundreds of spores can be inhaled per day. While the physiological role of macrophages and neutrophils in this context is well-appreciated, the molecular mechanisms that each of these cell types use to combat each stage of fungal pathogenesis are not fully understood. The critical step in *A. fumigatus* pathogenesis is the transition from dormant spore to hyphal growth, causing tissue destruction. Here, we used a zebrafish larva-*A. fumigatus* infection model to identify COX-PGE_2 signaling as one mechanism that promotes control of this transition to invasive hyphae by both macrophages and neutrophils (Fig 7).

To investigate the role of COX signaling in phagocyte responses we used indomethacin, a pan-COX inhibitor, as well as COX1- and COX2-specific inhibitors. We find that activity of both enzymes promotes survival of *A. fumigatus*-infected larvae. Broadly, COX1 activity is involved in tissue homeostasis while COX2 is inducible and is involved in responses to inflammatory stimuli (6). However, evidence suggests that both isoforms are activated during inflammation. Mice lacking COX1 have impaired inflammatory responses (33), and COX1 is activated in response to LPS-induced inflammation in humans (34). Zebrafish have one functional isoform of COX1 and two functional orthologues of COX2: COX2a and COX2b (35). The role of COX1 in inflammatory responses in zebrafish is not fully understood, and the specificity of the chemical inhibitors for zebrafish COX2 isoforms are not know. Hence, we cannot conclude if phagocyte-mediated *A. fumigatus* control is via COX1, COX2a, COX2b, or a combination.

COX enzymes can produce prostaglandins in multiple cell types including epithelial cells, endothelial cells and fibroblasts, but infiltrating innate immune cells are the major source of these lipid signals during inflammation, including both macrophages (36) and neutrophils (11). In the current study, the source of prostaglandins is unknown. Both macrophages and neutrophils use COX signaling to combat *A. fumigatus*, however, we cannot rule out an additional role for other cell types in this signaling. One possibility is that PGE_2 mediates crosstalk between these different cell types.

We also do not yet know what downstream effector mechanisms are activated in neutrophils and macrophages by COX signaling to target fungal growth. Prostaglandins can mediate endothelial

cell permeability and facilitate immune cell infiltration, but we observe no difference in phagocyte recruitment when COX enzymes are inhibited (6, 37, 38). Prostaglandins can also regulate extracellular killing mechanisms in phagocytes such as reactive oxygen species (ROS) production, neutrophil degranulation, and extracellular trap (ET) formation (39-41). Further testing is required determine if these mechanisms are enhanced by COX signaling during infection with *A. fumigatus*.

COX enzymes catalyze the main regulatory step of prostaglandin synthesis: conversion of arachidonic acid to prostaglandin H_2 (PGH_2). PGH_2 is then converted to one of the four major types of prostaglandins, prostaglandin E_2 (PGE_2), prostaglandin D_2 (PGD_2), prostaglandin I_2 (PGI_2) and prostaglandin $F_{2\alpha}$ ($PGF_{2\alpha}$) via different synthases. Perhaps the most studied prostaglandin is PGE_2, due to its paradoxical immunomodulatory effects (42). PGE_2 signals via four different receptors, EP1-EP4 which have different affinities for PGE_2, and activate different downstream effects (26). PGE_2 binds to EP2 with low affinity and generally evokes pro-inflammatory responses while it binds to EP4 with high affinity and activates anti-inflammatory responses (26). Therefore, the downstream effects of PGE_2, whether pro- or anti-inflammatory, depend on local PGE_2 concentration—which is controlled by its short half-life and the rate of synthesis by COX enzymes—and the cell type and EP receptor availability at the receiving end (42, 43).

We report here that PGE_2 signaling, specifically through the EP2 receptor, promotes phagocyte control of *A. fumigatus* invasive hyphal growth. However, it was previously reported that PGE_2 suppresses phagocytosis and microbial killing of fungal pathogens such as *P. brasiliensis* (12),

364 *C. albicans* (13) and *C. neoformans* (14). These differences underline the idea that PGE_2 can
365 have both pro- or anti-inflammatory functions, can differentially impact diverse fungi, and that
366 PGE_2 levels must be tightly controlled during infection to promote infection clearance.
367 Consistent with this idea, we report that while the effect of indomethacin on the control of fungal
368 germination can be rescued by PGE_2 supplementation, exogenous PGE_2 in untreated infected
369 larvae increases fungal growth. This could be due to elevated levels of PGE_2 activating anti-
370 inflammatory pathways and suppressing immune cell-mediated fungal growth control. In line
371 with this possibility, PGE_2 can drive resolution of inflammatory phenotypes through EP4 in
372 zebrafish larvae during injury (28). Alternatively, the exogenous PGE_2 might directly act upon *A.*
373 *fumigatus* to promote germination. A previous study showed that exogenous PGE_2 inhibited
374 pigment formation in *A. fumigatus* hyphae which could affect invasive hyphal growth (24).
375
376 Fungal species can also synthesize their own lipid signaling molecules to modulate pathogenesis
377 and immune responses (44, 45). For instance, *Cryptococcus neoformans* strains deficient in
378 eicosanoid production have intracellular growth defects, which can be reversed by addition of
379 exogenous PGE_2 in a zebrafish larvae model (27). *A. fumigatus* PpoA and PpoC enzyme activity
380 can produce prostaglandins and similar bioactive oxylipins that can affect *Aspergillus* virulence
381 and development (24) and phagocytosis of conidia (46). However, we find that *A. fumigatus* Ppo
382 enzymes do not affect fungal virulence in this larval zebrafish infection model, and that
383 indomethacin treatment does not alter *A. fumigatus* spore germination *in vitro*.
384
385 Overall, PGE_2 signaling must be well-orchestrated to elicit the desired anti- or pro-inflammatory
386 effects. Hematopoietic stem cell transplant patients who are at high risk of developing IA harbor

elevated levels of PGE_2 (47), suggesting that modulating PGE_2 or the downstream effects of PGE_2 signaling may be a possible target for increasing control of these infections in patients. This study provides a first step towards understanding the function of this signaling in immune-mediated control of *A. fumigatus* infection.

Materials and Methods

Ethics Statement

Adult and larval zebrafish were maintained and handled according to protocols approved by the Clemson University Institutional Animal Care and Use Committee (AUP2018-070, AUP2019-012, and AUP2019-032). Buffered tricaine was used for anesthesia prior to any experimental manipulation of larvae. Adult zebrafish were euthanized with buffered tricaine and zebrafish embryos and larvae were euthanized at 4°C.

Zebrafish lines and maintenance

Zebrafish adults were maintained at 28ºC at 14/10 hr light/dark cycles. All mutant and transgenic fish lines used in this study are listed in Table 1 and were maintained in the AB background. Upon natural spawning, embryos were collected and maintained in E3 medium with methylene blue at 28ºC. Embryos were manually dechorionated and anesthetized in 0.3 mg/mL buffered tricaine prior to any experimental manipulations. Larvae used for imaging were exposed to 200 µM N-phenylthiourea (PTU) starting at 24 hpf to inhibit pigment formation. Transgenic larvae were screened for fluorescence prior to experimentation. The *irf8* mutant line was maintained by outcrossing. *irf8*$^{+/-}$ adults with fluorescent neutrophils (*Tg(mpx:mCherry)*) were in-crossed to

generate *irf8*$^{+/+}$, *irf8*$^{+/-}$ and *irf8*$^{-/-}$ larvae, and these larvae were screened for a high number of neutrophils to select *irf8*$^{-/-}$ individuals (48). Genotypes were additionally confirmed at the end of the experiment where possible.

Table 1. Zebrafish lines used in this study.

Zebrafish line	Reference
irf8$^{-/-}$	(48)
Tg(mpeg1:H2B-GFP)	(49)
Tg(mpeg1:H2B-mCherry)	(50)
Tg(mfap4:mTurquoise2)	(51)
Tg(lyz:BFP)	(20)
Tg(mpx:mCherry)	(52)
Tg(mpx:mCherry-2A-rac2D57N)	(30)

Aspergillus fumigatus strains

Most experiments used Af293-derived strains TBK1.1 expressing YFP (19) or TBK5.1 expressing mCherry (20). Both of these strains behave like the parental Af293 strain in larval zebrafish (20). To test neutrophil-mediated killing, GFP-expressing TFYL49.1 (53) which was derived from the faster germinating CEA10 strain was used.

A Δ*ppoA*, Δ*ppoB*, Δ*ppoC* triple-mutant strain (Δ*ppo*, TMN31.10) was used to test the role of fungal oxylipins. In these experiments the control comparison strain used was wild-type Af293. Briefly, a previously published Af293 Δ*ppoC pyrG1* strain TDWC3.4 (24) was used as the parental strain in which *ppoA* and *ppoB* were subsequently deleted, using the *A. parasiticus pyrG* marker and recyclable hygromycin resistance marker *hph* (54), respectively. All primers used for

strain construction and confirmation are listed in S1 Table. DNA transformation constructs were created through double-joint PCR using published protocols (55). Protoplast generation and transformation were performed according to the previously published protocol (56). All transformants were first screened through PCR for incorporation of the construct and absence of the *ppo* gene. Southern blotting followed by hybridization of αP^{32}-dCTP labeled 5´ and 3´ flank regions were used to confirm transformants with single integration (S2 Fig). The *ppoA* deletion construct was amplified from pDWC4.2 (GF ppoA del Cassette F and GF ppoA del Cassette R) and used to transform TDWC3.4, resulting in the prototroph Af293 Δ*ppoC* Δ*ppoA* TMN20. A deletion cassette for *ppoB* was constructed by fusing ~1 kb 5´ and 3´ flanking regions of the gene with the recyclable hygromycin B resistance gene *hph* from pSK529. *ppoB* deletion cassette was used to transform TMN20.11, resulting in the *ppo* triple deletion mutant TMN31. TMN31 transformants were subsequently grown on minimal medium with 0.1% xylose to recycle the hygromycin B marker.

Spore preparation for injections

For injection preparation, 10^6 spores were spread on solid glucose minimal media (GMM) 10 cm plates and grown at 37ºC for 3-4 days. Spores were harvested by scraping using a disposable L-spreader and sterile water with 0.01% Tween. This spore suspension was passed through two layers of sterile miracloth into a 50 mL conical tube and topped to 50 mL. Spores were pelleted by centrifugation at 900 g for 10 min. The pellet was resuspended and washed in 50 mL of sterile PBS. The spores were again pelleted, resuspended in 5 mL of PBS, and filtered through another two layers of miracloth into a new conical tube. Spore concentration was enumerated using a

hemocytometer. A final spore suspension of 1.5 X 10^8/ mL was made in PBS and stored at 4ºC for up to ~1 month.

Live-dead spore labeling

Spores of *A. fumigatus* strain TBK1.1 were coated with AlexaFluor546 as described previously (20, 32). Briefly, isolated spores were incubated with biotin-XX, SSE (Molecular Probes) in the presence of 0.05 M $NaHCO_3$ at 4ºC for 2 hours. Spores were pelleted, washed first with 100 mM Tris-HCl at pH 8.0 to deactivate free-floating biotin and next with PBS, followed by incubation with streptavidin-AlexaFluor546 (Invitrogen). Spore concentration was enumerated and resuspended in PBS at 1.5 X 10^8/ mL. Labeling was confirmed with fluorescence microscopy prior to injections.

Zebrafish hindbrain microinjections

Larvae were injected with spores as described previously (16). Prepared spore suspensions at 1.5 X 10^8/ mL were mixed at 2:1 with filter-sterilized 1% phenol red to achieve a final spore concentration of 1 X 10^8/ mL. Injection plates were made with 2% agarose in E3 and coated with filter-sterilized 2% bovine serum albumin (BSA) prior to injections. Anesthetized 2 days post fertilization (dpf) larvae were placed on the agarose on their lateral side. A microinjection setup supplied with pressure injector, micromanipulator, micropipet holder, footswitch and back pressure unit (Applied Scientific Instrumentation) was used to inject 30-50 spores into the hindbrain ventricle of each larva. Larvae were injected with PBS as a mock-infection control. After injections, larvae were rinsed at least twice with E3 without methylene blue to remove

tricaine and any free spores and were transferred to 96-well plates for survival and CFU experiments and to 48-well plates for imaging experiments.

Clodronate liposome injections

Tg(mpeg1:H2B-GFP) larvae at 1.5 dpf were manually dechorionated and screened for GFP expression. 50 µL of clodronate or PBS liposomes (Liposoma) was mixed with 5 µL of filter-sterilized 1% phenol red and 2 nL was intravenously injected into the caudal vein plexus of GFP-positive larvae. After 24 hours, depletion of macrophages was confirmed by loss of GFP signal by screening with a fluorescent zoomscope (Zeiss SteREO Discovery.V12 PentaFluar with Achromat S 1.0x objective) prior to *A. fumigatus* infections.

Morpholino injections

A *pu.1* (*spi1b*) morpholino oligonucleotide (MO) was previously published and validated (5'-GATATACTGATACTCCATTGGTGGT-3') (ZFIN MO1-spi1b) (29) (GeneTools). Stock solutions were made by resuspension in water to 1 mM and kept at 4°C. For injections, the stock was diluted to 0.5 mM in water with 0.1% filter-sterilized phenol red and 0.5X CutSmart Buffer (New England Biolabs). A standard control MO (GeneTools) at 0.5 mM was used as an injection control. 3 nl of injection mix was injected into the yolk of 1-2 cell stage embryos. Efficacy of *pu.1* knockdown was determined by injecting MO into a macrophage-labeled zebrafish line and larvae were checked for fluorescence expression prior to *A. fumigatus* infections.

Drug treatments

Infected larvae were exposed to the pan-COX inhibitor indomethacin (Sigma-Aldrich) at 10 µM, COX1 inhibitor SC560 (Cayman Chemical) at 5 µM, COX2 inhibitor meloxicam (Cayman Chemical) at 15 µM, EP2 receptor antagonist AH6809 (Cayman Chemical) at 5 µM or EP4 receptor antagonist AH23848 (Cayman Chemical) at 10 µM. These drugs were previously used in zebrafish larvae (21-23, 27, 28). The indomethacin concentration used was based on published results. For all other drugs, multiple concentrations were tested and the highest concentration of each drug that did not cause lethality or edema in uninfected larvae was used. 1000X stock solutions were made in DMSO and 0.1% DMSO was used as a vehicle control. After rinsing infected larvae, pre-mixed E3 with drug was added to dishes containing larvae. For survival and CFU assays, larvae were transferred to 96-well plates, one larva/well in 200 µL of drug/vehicle solution. For imaging experiments, larvae were transferred to 48-well plates with 500 µL of solution. All larvae were kept in the same drug solution for the entirety of the experiment unless otherwise noted.

PGE_2 rescue injections

A stock solution of 10 mM PGE_2 (Cayman Chemical) was made in DMSO (23, 27). Prior to injection, the stock was diluted 100X in PBS and 1 µL was mixed with 9 µL of 1% phenol red for a final concentration of 10 µM. Wild-type larvae were injected with *A. fumigatus* and exposed to 10 µM indomethacin or DMSO vehicle control in 10 mL of E3 in 60 mm petri dishes. At 1 dpi, larvae were anesthetized and injected with 1 nL of 10 µM PGE_2 or 0.1% DMSO into the hindbrain. After injections, indomethacin or DMSO control treatments were renewed, and larvae were transferred to 96-well plates for survival and 48-well plates for imaging experiments.

CFU counts

Single larvae were placed in 1.7 mL microcentrifuge tubes in 90 µl PBS containing 1 mg/mL ampicillin and 0.5 mg/mL kanamycin, homogenized in a tissue lyser (Qiagen) at 1800 oscillations/min (30 Hz) for 6 min and spun down at 17000 g for 30 seconds. The whole suspension was spread on a GMM plate and incubated for 3 days at 37ºC and the number of fungal colonies were counted. For all survival experiments, 8 larvae from each condition were plated immediately after injection to confirm actual injection dose and these numbers are reported in all figure legends. For CFU experiments to monitor fungal burden over time, 8 larvae were plated for each condition, each day and CFU counts were normalized to the average initial injection dose for that condition and graphed as percent initial spore burden.

Live imaging

For daily imaging and PGE_2 rescue experiments, individual larvae were removed from 48-well plates, anesthetized in tricaine and transferred to a zWEDGI device (57, 58). Larvae were imaged using a Zeiss Cell Observer Spinning Disk confocal microscope on a Axio Obsever 7 microscope stand with a confocal scanhead (Yokogawa CSU-X) and a Photometrics Evolve 512 EMCCD camera. A Plan-Apochromat 20x objective (0.8 NA) and ZEN software were used to acquire Z-stack images of the hindbrain area with 5 µm distance between slices. After imaging, larvae were rinsed with 200 µM PTU in E3 and put back in the same well (16). For AlexaFluor labeled live-dead staining, infected larvae at 2 dpi were mounted in 1% low-melting point agarose (Fisher BioReagents) in a 35mm glass-bottom dish (Greiner) and oriented laterally.

Images were acquired using the same spinning disk confocal microscope with an EC Plan-Neofluar 40x objective (0.75 NA) with 2.5 µm distance between slices.

Image analysis

All images were analyzed using Image J/Fiji (59). Presence of germination and invasive hyphae were manually analyzed. Any kind of hyphal growth, whether single or branched was considered an incidence of germination, while the presence of branched hyphae was considered an incidence of invasive hyphae. Maximum intensity projections were used to measure the 2D fungal area after thresholding the fluorescent intensity. The number of recruited phagocytes were counted across z-stacks using the Cell Counter plugin. For 2D phagocyte cluster area, the polygon selection tool was used to select and measure the area of macrophage cluster from maximum intensity projection of z-stacks. Images from the same experiments were used to quantify incidence of germination and invasive hyphae, fungal area, and phagocyte recruitment. To quantify live versus dead spores, images were blinded and processed with bilinear interpolation to increase pixel density two-fold. Cell Counter was used to manually count the number of live and dead spores in z-slices. All displayed images were processed in Fiji with bilinear interpolation to increase pixel density two-fold and are displayed as maximum intensity projections of z-stacks. Live versus dead spore images were additionally processed with a gaussian blur (radius = 1) to reduce noise.

Aspergillus fumigatus in vitro germination assay

1 X 10^6 TBK1.1 spores were inoculated into a flask containing 3 ml RPMI 1640 medium with HEPES (Gibco) containing 2% glucose in a 37ºC shaker at 100 rpm in triplicate. Every 2 hours, 10 µL of the spore suspension was pipetted on to a microscope slide with a cover glass and imaged under the same Zeiss spinning disk confocal microscope using a Plan-Apochromat 20x objective (0.8 NA). At least 10 fields were captured for each sample at each time point and imaging was continued until 8 hours post seeding. These images were blinded prior to analysis and the number of germinated and non-germinated spores were counted using the Fiji Cell Counter plugin.

Statistical analysis

For all experiments, pooled data from at least three independent replicates were generated and total pooled Ns are given in each figure. Statistical analyses were performed using R version 4.1.0 and graphs were generated using GraphPad Prism version 7 (GraphPad Software). Larval survival data and cumulative appearance of larvae with germination or invasive hyphae were analyzed by Cox proportional hazard regression. Calculated experimental P values and hazard ratios (HR) are displayed in each figure. HR defines how likely larvae in a particular condition will succumb to the infection compared to control larvae. Occasionally, the indomethacin drug lost efficacy and did not cause the previously observed and confirmed survival defect. Any such replicates were omitted from the final statistical analysis. CFU counts, spore killing, fungal area, phagocyte numbers and cluster area, and comparisons of day of onset of germination and invasive hyphae were analyzed with analysis of variance (ANOVA). For each condition, estimated marginal means (emmeans) and standard error (SEM) were calculated and pairwise

577 comparisons were performed with Tukey's adjustment. The graphs of number of phagocytes,
578 phagocyte cluster area and 2D fungal area over the infection period show values from individual
579 larvae over time as individual lines, and bars represent pooled emmeans ± SEM. Data points in
580 dot plots represent individual larvae and are color-coded based on replicate and bars represent
581 pooled emmeans ± SEM. For the *in vitro* germination assay, data were pooled from two
582 independent replicates, each consisting of three technical replicates. Statistical analysis was
583 performed by Student's T-test with Holm-Sidak method using GraphPad Prism version 7, and
584 data points represent pooled means ± SEM.
585

586 Acknowledgments

587 We thank David Tobin for providing the *mfap4:mTurquoise2* zebrafish line. We thank Celia
588 Shiau for providing the *irf8* mutant zebrafish line. We thank Anna Huttenlocher for sharing all
589 other transgenic zebrafish lines. We thank members of the Rosowski Lab and Keller Lab for
590 helpful discussions.
591

References

1. Latge JP. Aspergillus fumigatus and aspergillosis. Clinical microbiology reviews. 1999;12(2):310-50.

2. Baddley JW. Clinical risk factors for invasive aspergillosis. Medical mycology. 2011;49 Suppl 1:S7-S12.

3. Denning DW. Invasive aspergillosis. Clinical infectious diseases. 1998;26(4):781-803.

4. Lin SJ, Schranz J, Teutsch SM. Aspergillosis case-fatality rate: systematic review of the literature. Clinical infectious diseases. 2001;32(3):358-66.

5. Gregg KS, Kauffman CA. Invasive Aspergillosis: Epidemiology, Clinical Aspects, and Treatment. Seminars in respiratory and critical care medicine. 2015;36(5):662-72.

6. Ricciotti E, FitzGerald GA. Prostaglandins and inflammation. Arteriosclerosis, thrombosis, and vascular biology. 2011;31(5):986-1000.

7. Funk CD. Prostaglandins and leukotrienes: advances in eicosanoid biology. Science (New York, NY). 2001;294(5548):1871-5.

8. Smith WL, DeWitt DL, Garavito RM. Cyclooxygenases: structural, cellular, and molecular biology. Annual review of biochemistry. 2000;69:145-82.

9. Vane JR. Inhibition of Prostaglandin Synthesis as a Mechanism of Action for Aspirin-like Drugs. Nature New Biology. 1971;231(25):232-5.

10. Williams CS, Mann M, DuBois RN. The role of cyclooxygenases in inflammation, cancer, and development. Oncogene. 1999;18(55):7908-16.

11. Tilley SL, Coffman TM, Koller BH. Mixed messages: modulation of inflammation and immune responses by prostaglandins and thromboxanes. Journal of Clinical Investigation. 2001;108(1):15-23.

12. Bordon AP, Dias-Melicio LA, Acorci MJ, Calvi SA, Serrão Peraçoli MT, Victoriano de Campos Soares AM. Prostaglandin E2 inhibits Paracoccidioides brasiliensis killing by human monocytes. Microbes and Infection. 2007;9(6):744-7.

13. Serezani CH, Kane S, Medeiros AI, Cornett AM, Kim SH, Marques MM, et al. PTEN directly activates the actin depolymerization factor cofilin-1 during PGE2-mediated inhibition of phagocytosis of fungi. Science signaling. 2012;5(210):ra12.

14. Shen L, Liu Y. Prostaglandin E2 blockade enhances the pulmonary anti-Cryptococcus neoformans immune reaction via the induction of TLR-4. International Immunopharmacology. 2015;28(1):376-81.

15. Rosowski EE. Illuminating Macrophage Contributions to Host-Pathogen Interactions In Vivo: the Power of Zebrafish. Infection and immunity. 2020;88(7).

16. Thrikawala S, Rosowski EE. Infection of Zebrafish Larvae with Aspergillus Spores for Analysis of Host-Pathogen Interactions. Journal of visualized experiments. 2020(159).

17. Traver D, Herbomel P, Patton EE, Murphey RD, Yoder JA, Litman GW, et al. The Zebrafish as a Model Organism to Study Development of the Immune System. Advances in Immunology. 2003;81:254-330.

18. Herbomel P, Thisse B, Thisse C. Ontogeny and behaviour of early macrophages in the zebrafish embryo. Development. 1999;126(17):3735-45.

19. Knox BP, Deng Q, Rood M, Eickhoff JC, Keller NP, Huttenlocher A. Distinct innate immune phagocyte responses to Aspergillus fumigatus conidia and hyphae in zebrafish larvae. Eukaryotic cell. 2014;13(10):1266-77.

636 20. Rosowski EE, Raffa N, Knox BP, Golenberg N, Keller NP, Huttenlocher A.
637 Macrophages inhibit Aspergillus fumigatus germination and neutrophil-mediated fungal killing.
638 PLoS pathogens. 2018;14(8):e1007229.
639 21. Tyrkalska SD, Candel S, Angosto D, Gomez-Abellan V, Martin-Sanchez F, Garcia-
640 Moreno D, et al. Neutrophils mediate Salmonella Typhimurium clearance through the GBP4
641 inflammasome-dependent production of prostaglandins. Nature communications. 2016;7:12077.
642 22. Jin D, Ni TT, Sun J, Wan H, Amack JD, Yu G, et al. Prostaglandin signalling regulates
643 ciliogenesis by modulating intraflagellar transport. Nature cell biology. 2014;16(9):841-51.
644 23. Lewis A, Elks PM. Hypoxia Induces Macrophage tnfa Expression via Cyclooxygenase
645 and Prostaglandin E2 in vivo. Frontiers in immunology. 2019;10:2321.
646 24. Tsitsigiannis DI, Bok JW, Andes D, Nielsen KF, Frisvad JC, Keller NP. Aspergillus
647 cyclooxygenase-like enzymes are associated with prostaglandin production and virulence.
648 Infection and immunity. 2005;73(8):4548-59.
649 25. Kupfahl C, Tsikas D, Niemann J, Geginat G, Hof H. Production of prostaglandins,
650 isoprostanes and thromboxane by Aspergillus fumigatus: identification by gas chromatography-
651 tandem mass spectrometry and quantification by enzyme immunoassay. Molecular immunology.
652 2012;49(4):621-7.
653 26. Hata AN, Breyer RM. Pharmacology and signaling of prostaglandin receptors: multiple
654 roles in inflammation and immune modulation. Pharmacol Ther. 2004;103(2):147-66.
655 27. Evans RJ, Pline K, Loynes CA, Needs S, Aldrovandi M, Tiefenbach J, et al. 15-keto-
656 prostaglandin E2 activates host peroxisome proliferator-activated receptor gamma (PPAR-
657 gamma) to promote Cryptococcus neoformans growth during infection. PLoS pathogens.
658 2019;15(3):e1007597.

659 28. Loynes CA, Lee JA, Robertson AL, Steel MJ. PGE(2) production at sites of tissue injury
660 promotes an anti-inflammatory neutrophil phenotype and determines the outcome of
661 inflammation resolution in vivo. Science advances. 2018;4(9):eaar8320.
662 29. Rhodes J, Hagen A, Hsu K, Deng M, Liu TX, Look AT, et al. Interplay of pu.1 and gata1
663 determines myelo-erythroid progenitor cell fate in zebrafish. Developmental cell. 2005;8(1):97-
664 108.
665 30. Deng Q, Yoo SK, Cavnar PJ, Green JM, Huttenlocher A. Dual roles for Rac2 in
666 neutrophil motility and active retention in zebrafish hematopoietic tissue. Developmental cell.
667 2011;21(4):735-45.
668 31. Knox BP, Blachowicz A, Palmer JM, Romsdahl J, Huttenlocher A, Wang CC, et al.
669 Characterization of Aspergillus fumigatus Isolates from Air and Surfaces of the International
670 Space Station. mSphere. 2016;1(5).
671 32. Jhingran A, Mar KB, Kumasaka DK, Knoblaugh SE, Ngo LY, Segal BH, et al. Tracing
672 conidial fate and measuring host cell antifungal activity using a reporter of microbial viability in
673 the lung. Cell reports. 2012;2(6):1762-73.
674 33. Langenbach R, Morham SG, Tiano HF, Loftin CD, Ghanayem BI, Chulada PC, et al.
675 Prostaglandin synthase 1 gene disruption in mice reduces arachidonic acid-induced inflammation
676 and indomethacin-induced gastric ulceration. Cell. 1995;83(3):483-92.
677 34. McAdam BF, Mardini IA, Habib A, Burke A, Lawson JA, Kapoor S, et al. Effect of
678 regulated expression of human cyclooxygenase isoforms on eicosanoid and isoeicosanoid
679 production in inflammation. The Journal of clinical investigation. 2000;105(10):1473-82.

680 35. Ishikawa TO, Griffin KJ, Banerjee U, Herschman HR. The zebrafish genome contains
681 two inducible, functional cyclooxygenase-2 genes. Biochemical and biophysical research
682 communications. 2007;352(1):181-7.
683 36. Harizi H. The Immunobiology of Prostanoid Receptor Signaling in Connecting Innate
684 and Adaptive Immunity. BioMed research international. 2013;2013:683405.
685 37. Martínez-Colón GJ, Moore BB. Prostaglandin E(2) as a Regulator of Immunity to
686 Pathogens. Pharmacol Ther. 2018;185:135-46.
687 38. Medeiros A, Peres-Buzalaf C, Fortino Verdan F, Serezani CH. Prostaglandin E2 and the
688 suppression of phagocyte innate immune responses in different organs. Mediators of
689 inflammation. 2012;2012:327568.
690 39. Shishikura K, Horiuchi T, Sakata N, Trinh DA, Shirakawa R, Kimura T, et al.
691 Prostaglandin E2 inhibits neutrophil extracellular trap formation through production of cyclic
692 AMP. British journal of pharmacology. 2016;173(2):319-31.
693 40. Rossi AG, O'Flaherty JT. Prostaglandin binding sites in human polymorphonuclear
694 neutrophils. Prostaglandins. 1989;37(6):641-53.
695 41. Serezani CH, Chung J, Ballinger MN, Moore BB, Aronoff DM, Peters-Golden M.
696 Prostaglandin E2 suppresses bacterial killing in alveolar macrophages by inhibiting NADPH
697 oxidase. American journal of respiratory cell and molecular biology. 2007;37(5):562-70.
698 42. Kalinski P. Regulation of immune responses by prostaglandin E2. Journal of
699 immunology. 2012;188(1):21-8.
700 43. Goodwin JS, Ceuppens J. Regulation of the immune response by prostaglandins. Journal
701 of clinical immunology. 1983;3(4):295-315.

44. Mendoza SR, Zamith-Miranda D, Takács T, Gacser A, Nosanchuk JD, Guimarães AJ. Complex and Controversial Roles of Eicosanoids in Fungal Pathogenesis. Journal of fungi (Basel, Switzerland). 2021;7(4):254.

45. Erb-Downward JR, Noverr MC. Characterization of prostaglandin E2 production by Candida albicans. Infection and immunity. 2007;75(7):3498-505.

46. Dagenais TR, Chung D, Giles SS, Hull CM, Andes D, Keller NP. Defects in conidiophore development and conidium-macrophage interactions in a dioxygenase mutant of Aspergillus fumigatus. Infection and immunity. 2008;76(7):3214-20.

47. Cayeux SJ, Beverley PC, Schulz R, Dörken B. Elevated plasma prostaglandin E2 levels found in 14 patients undergoing autologous bone marrow or stem cell transplantation. Bone marrow transplantation. 1993;12(6):603-8.

48. Shiau CE, Kaufman Z, Meireles AM, Talbot WS. Differential requirement for irf8 in formation of embryonic and adult macrophages in zebrafish. PloS one. 2015;10(1):e0117513.

49. Miskolci V, Squirrell J, Rindy J, Vincent W, Sauer JD, Gibson A, et al. Distinct inflammatory and wound healing responses to complex caudal fin injuries of larval zebrafish. eLife. 2019;8:e45976.

50. Vincent WJ, Freisinger CM, Lam PY, Huttenlocher A, Sauer JD. Macrophages mediate flagellin induced inflammasome activation and host defense in zebrafish. Cellular microbiology. 2016;18(4):591-604.

51. Walton EM, Cronan MR, Beerman RW, Tobin DM. The Macrophage-Specific Promoter mfap4 Allows Live, Long-Term Analysis of Macrophage Behavior during Mycobacterial Infection in Zebrafish. PloS one. 2015;10(10):e0138949.

724 52. Yoo SK, Deng Q, Cavnar PJ, Wu YI, Hahn KM, Huttenlocher A. Differential Regulation
725 of Protrusion and Polarity by PI(3)K during Neutrophil Motility in Live Zebrafish.
726 Developmental cell. 2010;18(2):226-36.
727 53. Lim FY, Ames B, Walsh CT, Keller NP. Co-ordination between BrlA regulation and
728 secretion of the oxidoreductase FmqD directs selective accumulation of fumiquinazoline C to
729 conidial tissues in Aspergillus fumigatus. Cellular microbiology. 2014;16(8):1267-83.
730 54. Hartmann T, Dümig M, Jaber BM, Szewczyk E, Olbermann P, Morschhäuser J, et al.
731 Validation of a self-excising marker in the human pathogen Aspergillus fumigatus by employing
732 the beta-rec/six site-specific recombination system. Applied and environmental microbiology.
733 2010;76(18):6313-7.
734 55. Lim FY, Sanchez JF, Wang CC, Keller NP. Toward awakening cryptic secondary
735 metabolite gene clusters in filamentous fungi. Methods in enzymology. 2012;517:303-24.
736 56. Szewczyk E, Nayak T, Oakley CE, Edgerton H, Xiong Y, Taheri-Talesh N, et al. Fusion
737 PCR and gene targeting in Aspergillus nidulans. Nat Protoc. 2006;1(6):3111-20.
738 57. Huemer K, Squirrell JM, Swader R, LeBert DC, Huttenlocher A, Eliceiri KW. zWEDGI:
739 Wounding and Entrapment Device for Imaging Live Zebrafish Larvae. Zebrafish. 2017;14(1):42-
740 50.
741 58. Huemer K, Squirrell JM, Swader R, Pelkey K, LeBert DC, Huttenlocher A, et al. Long-
742 term Live Imaging Device for Improved Experimental Manipulation of Zebrafish Larvae.
743 Journal of Visualized Experiments. 2017(128).
744 59. Schindelin J, Arganda-Carreras I, Frise E, Kaynig V, Longair M, Pietzsch T, et al. Fiji: an
745 open-source platform for biological-image analysis. Nature methods. 2012;9(7):676-82.
746

Figure legends

Fig. 1. Host cyclooxygenase signaling promotes survival of *A. fumigatus*-infected larvae. (A) Survival of wild-type larvae injected at 2 dpf with TBK1.1 (Af293) *A. fumigatus* spores or PBS mock injection in the presence of 10 μM indomethacin or DMSO vehicle control. **(B)** Survival of larvae injected at 2 dpf with *A. fumigatus* Af293 or Af293 triple-*ppo*-mutant (Δ*ppo*) spores and exposed to 10 μM indomethacin or DMSO vehicle control. **(C)** Survival of larvae injected at 2 dpf with TBK1.1 (Af293) spores and exposed to 10 μM indomethacin, 5 μM AH6809, 10 μM AH23848, or DMSO vehicle control. Data are pooled from at least three independent replicates and the total larval N per condition is indicated in each figure. Cox proportional hazard regression analysis was used to calculate P values and hazard ratios (HR). Average injection CFUs: (A) 50, (B) Af293 = 40 and Δ*ppo* = 58, (C) 28.

Fig. 2. Cyclooxygenase-mediated host protection depends on phagocytes. Survival of larvae injected with TBK1.1 (Af293) spores at 2 dpf. **(A)** Development of phagocytes was inhibited by *pu.1* morpholino (MO). Control larvae received standard control MO. **(B)** Macrophages were depleted via clodronate liposome i.v. injection at 1 dpf. Control larvae received PBS liposomes. **(C)** Neutrophil-defective larvae (*mpx*:*rac2D57N*) were compared to wild-type larvae. Data are pooled from three independent replicates and the total larval N per condition is indicated in each figure. Cox proportional hazard regression analysis was used to calculate P values and hazard ratios (HR). Average injection CFUs: (A) control MO = 25, *pu.1* MO = 24, (B) PBS liposomes = 20, clodronate liposomes = 23, (C) wild-type = 26, *mpx*:*rac2D57N* = 22.

Fig. 3. Cyclooxygenase inhibition does not alter phagocyte recruitment. Larvae were injected with mCherry-expressing *A. fumigatus* TBK5.1 (Af293) spores at 2 dpf. After injection larvae were exposed to 10 μM indomethacin or DMSO vehicle control and were imaged through 5 dpi. **(A)** Schematic showing the infection and imaging area of zebrafish larvae. **(B, D, E, G)** Macrophage nuclear-labeled *Tg(mpeg1:H2B-GFP)* larvae were imaged at 1, 2, 3, and 5 dpi. **(C, F, H)** Neutrophil-labeled *Tg(lyz:BFP)* larvae were imaged at 2, 3, and 5 dpi. (B, C) Representative z-projection images showing macrophage and neutrophil recruitment. Scale bars = 50 μm. (D) Number of macrophages recruited, (E) 2D macrophage cluster area, and (F) number of neutrophils recruited were quantified. Each line represents an individual larva followed for the entire course of infection and bars represent pooled emmeans ± SEM from four independent replicates, at least 12 larvae per condition, per replicate. P values were calculated by ANOVA. (G) Number of macrophages and (H) neutrophils one day before germination occurred, on the day of germination, and on the day invasive hyphae occurred were quantified. Bars represent pooled emmeans ± SEM from all larvae with germination from four independent replicates. Data points represent individual larva and are color coded by replicate. P values were calculated by ANOVA.

Fig. 4. Cyclooxygenase inhibition does not affect spore killing. (A, B) Macrophage-labeled larvae *Tg(mfap4:mTurquoise2)* were injected with YFP-expressing *A. fumigatus* TBK1.1 (Af293) spores coated with AlexaFluor 546 at 2 dpf, exposed to 10 μM indomethacin or DMSO vehicle control, and imaged at 2 dpi. (A) Representative images showing live (white arrow) and dead (open arrow) spores within a macrophage. Scale bar = 10 μm. Z projection of three slices. (B) The percentage of live spores in the hindbrain, and specifically within macrophages, per

793 larvae. Each data point represents an individual larvae, color-coded by replicate (indomethacin n
794 = 31, DMSO n = 30). Bars represent pooled emmeans ± SEM from three independent replicates,
795 P values calculated by ANOVA. **(C)** Wild-type larvae were injected with TBK1.1 (Af293)
796 spores at 2 dpf, exposed to 10 μM indomethacin or DMSO vehicle control, and fungal burden
797 was quantified by homogenizing and plating individual larvae for CFUs at multiple days post
798 injection. Eight larvae per condition, per dpi, per replicate were quantified, and the number of
799 CFUs at each dpi is represented as a percentage of the initial spore burden. Bars represent pooled
800 emmeans ± SEM from three individual replicates, P values calculated by ANOVA. Average
801 injection CFUs: 27.
802
803 **Fig. 5. Cyclooxygenase inhibition decreases immune control of fungal germination and**
804 **invasive hyphal growth.** Zebrafish larvae were injected with mCherry-expressing TBK5.1
805 (Af293) spores at 2 dpf, exposed to 10 μM indomethacin or DMSO vehicle control and imaged
806 at 1, 2, 3, and 5 dpi. **(A)** Representative images showing spore germination (inset white arrow)
807 and invasive hyphae (branched hyphae, inset open white arrow). Scale bar = 50 μm (10 μm in
808 insets). **(B)** Cumulative percentage of larvae with germination (dotted line) and invasive hyphae
809 (solid line) through 5 dpi. Cox proportional hazard regression analysis was used to calculate P
810 values. **(C)** 2D fungal area was quantified from image z projections. Each line represents an
811 individual larva and bars represent pooled emmeans ± SEM from 8 independent replicates, at
812 least 12 larvae per condition, per replicate. **(D)** Severity of fungal growth was scored for all
813 larvae and displayed as a heatmap. Representative images for each score can be found in S5 Fig.
814 **(E-G)** In larvae in which (E) germination (indomethacin n = 61, DMSO n = 45) and (F) invasive
815 hyphae occurred (indomethacin n = 42, DMSO n = 27), the day on which each was first observed

816 is plotted. (G) The number of days between germination and invasive hyphae was also
817 calculated. Bars represent pooled emmeans ± SEM from eight individual replicates, P values
818 calculated by ANOVA. Each data point represents an individual larvae, color-coded by replicate.
819
820 **Fig. 6. Exogenous PGE_2 can rescue the indomethacin-mediated increase in fungal**
821 **germination and hyphal growth.** Larvae were injected with mCherry-expressing TBK5.1
822 (Af293) spores and exposed to 10 μM indomethacin or DMSO vehicle control at 2 dpf. At 1 dpi,
823 larvae were injected with 10 μM PGE_2 or DMSO vehicle control. **(A)** Survival of wild-type
824 larvae was monitored. Cox proportional hazard regression analysis was used to calculate P
825 values and hazard ratios (HR). Data are pooled from four independent replicates, and total larval
826 N per condition is indicated in figure. Average injection CFUs: 40. **(B-D)** Larvae were imaged at
827 3 dpi. (B) Percentage of larvae with germination and invasive hyphae, and (C) 2D fungal area in
828 each condition. Data pooled from three independent replicates, at least 8 larvae per condition, per
829 replicate, P values calculated by ANOVA. (C) Bars represent pooled emmeans ± SEM. (D)
830 Representative images showing hyphal growth in each condition. Scale bars = 50 μm.
831
832 **Fig. 7. Model of cyclooxygenase signaling in response to *A. fumigatus* growth.** COX enzymes
833 produce prostaglandin signaling molecule, including PGE_2. PGE_2 can bind to the EP2 receptor to
834 exert pro-inflammatory effects. Zebrafish larvae injected with *A. fumigatus*, this signaling
835 activates both macrophages and neutrophils to inhibit spore germination and development of
836 invasive hyphal growth.
837

Supporting Information

S1. Fig. Both cyclooxygenase-1 and -2 signaling contribute to survival of infected larvae. Larvae were injected with TBK1.1 (Af293) *A. fumigatus* spores at 2 dpf and were exposed to (A) 5 μM SC560, (B) 15 μM meloxicam, or DMSO vehicle control. Survival was monitored for 7 days. Cox proportional hazard regression analysis was used to calculate P values and hazard ratios (HR). Data are pooled from three independent experiments and the total larvae number is indicated in each figure. Average injection CFUs: (A) 35, (B) 30.

S2. Fig. Southern blot analyses of strains created in this study. Confirmation of (A) TMN20 Af293 Δ*ppoC* Δ*ppoA* double mutant and (B) TMN31 Af293 Δ*ppoC* Δ*ppoA* Δ*ppoB* triple mutant. Restriction enzyme digestion, southern blotting and hybridization were performed as mentioned in the Materials and Methods. Double and triple *ppo* mutants were created in sequence. Hybridization of αP^{32}-dCTP labeled 5´ and 3´ flank regions were used to confirm transformants. The parental strain and the size of DNA fragments used to probe for southern blotting and hybridization are shown in each figure. P = parental strain; T = transformants.

S3. Fig. Survival of phagocyte-deficient larvae after PBS mock-infection. (A) Wild-type larvae injected with standard control MO or *pu.1* MO, (B) larvae injected with PBS liposomes or clodronate liposomes and (C) larvae with defective neutrophils (*mpx*:*rac2D57N)* or wild-type neutrophils were injected with PBS at 2 dpf. Survival was monitored in the presence of 10 μM indomethacin or DMSO vehicle control. Data are pooled from three independent experiments and Cox proportional hazard regression analysis was used to calculate P values and hazard ratios (HR).

S4. Fig. Indomethacin does not affect *A. fumigatus* spore germination *in vitro*. TBK1.1 (Af293) spores were inoculated into RPMI media in the presence of 10 μM indomethacin or DMSO vehicle control. Every 2 hours, an aliquot of spores was removed and scored for germination. Points represent pooled means ± SEM from two independent replicates and P values calculated by Student's T-test.

S5. Fig. Representative images of categories of *A. fumigatus* hyphal growth. Wild-type larvae were injected with mCherry-expressing TBK5.1 (Af293) spores, exposed to 10 uM indomethacin or DMSO vehicle control and imaged at 1, 2, 3, and 5 dpi. Incidences of hyphal growth were scored a value of 1-4 depending on the extent of hyphae. Category 1: presence of one germ tube (white arrow). Category 2: presence of branched hyphae (open white arrow), yet small fungal bolus. Category 3: presence of spread-out invasive hyphae. Category 4: presence of severe invasive hyphae and tissue damage. Scale bars = 50 μm or 10 μm.

S6. Fig. Indomethacin does not significantly impair neutrophil-mediated clearance of *A. fumigatus* hyphae. Macrophage-deficient *irf8*$^{-/-}$ or control (*irf8*$^{+/+}$ or *irf8*$^{+/-}$) larvae were injected with *A. fumigatus* TFYL49.1 (CEA10) strain and treated with 10 μM indomethacin or DMSO vehicle control. (A) Fungal burden was monitored by homogenizing individual larvae and quantifying CFUs at 1 and 2 dpi. CFUs from *irf8*$^{-/-}$ were normalized to CFUs of *irf8*$^{+/+}$/*irf8*$^{+/-}$ at each dpi for each condition. Data were pooled from four independent replicates and P values calculated by ANOVA. (B) Larvae were monitored for survival. Data are pooled from five

883 independent replicates and Cox proportional hazard regression analysis was used to calculate P
884 values and hazard ratios (HR). Average injection CFUs: *irf8*$^{+/+}$/*irf8*$^{+/-}$ = 26, *irf8*$^{-/-}$ = 20.
885
886 **S7. Fig. PGE_2 injection does not alter phagocyte recruitment or rescue survival of**
887 **neutrophil-defective larvae.** At 2 dpf, larvae were injected with TBK5.1 (Af293), followed by
888 injection of 10 μM PGE_2 or DMSO vehicle control at 3 dpf (1 dpi). The number of (A)
889 macrophages and (B) neutrophils were enumerated at 3 dpi. Data are pooled from three
890 independent replicates, at least 8 larvae per condition, per replicate. Each data point represents an
891 individual larva, color-coded by replicate. Bars represent pooled emmeans ± SEM and P values
892 were calculated by ANOVA. (C) Survival of injected and treated neutrophil-defective larvae
893 (*mpx*:*rac2D57N*) was monitored. Cox proportional hazard regression analysis was used to
894 calculate P values and hazard ratios (HR). Data are pooled from three replicates, at least 23
895 larvae per condition, per replicate. Average injection CFUs: 49.
896
897 **S1 Table. Primers used to construct *A. fumigatus* Δ*ppo* triple mutant strain.**

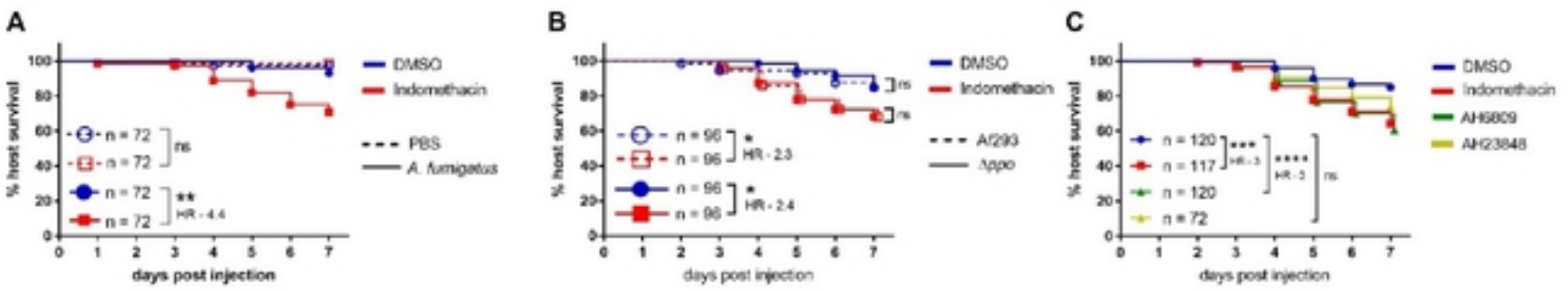

Fig. 1. Host cyclooxygenase signaling promotes survival of *A. fumigatus*-infected larvae. (A) Survival of wild-type larvae injected at 2 dpf with TBK1.1 (Af293) *A. fumigatus* spores or PBS mock injection in the presence of 10 μM indomethacin or DMSO vehicle control. **(B)** Survival of larvae injected at 2 dpf with *A. fumigatus* Af293 or Af293 triple-*ppo*-mutant (Δ*ppo*) spores and exposed to 10 μM indomethacin or DMSO vehicle control. **(C)** Survival of larvae injected at 2 dpf with TBK1.1 (Af293) spores and exposed to 10 μM indomethacin, 5 μM AH6809, 10 μM AH23848, or DMSO vehicle control. Data are pooled from at least three independent replicates and the total larval N per condition is indicated in each figure. Cox proportional hazard regression analysis was used to calculate P values and hazard ratios (HR). Average injection CFUs: (A) 50, (B) Af293 = 40 and Δ*ppo* = 58, (C) 28.

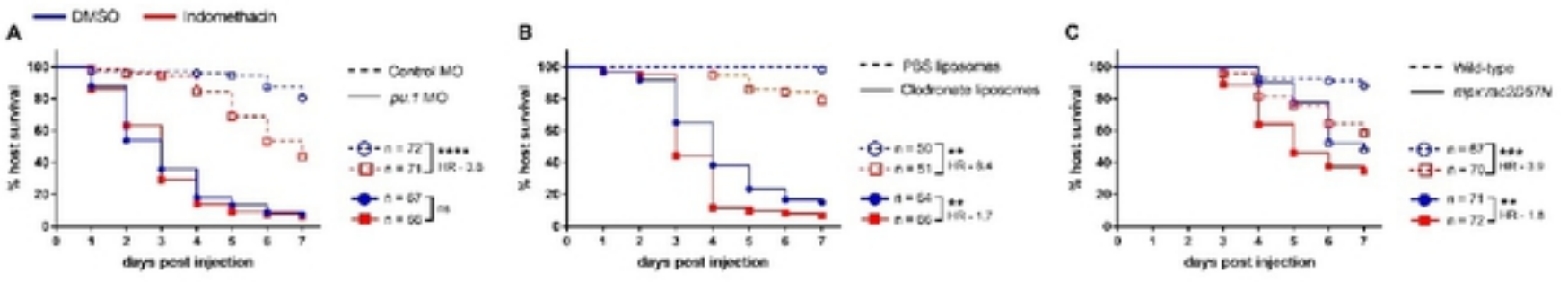

Fig. 2. Cyclooxygenase-mediated host protection depends on phagocytes. Survival of larvae

injected with TBK1.1 (Af293) spores at 2 dpf. **(A)** Development of phagocytes was inhibited by *pu.1* morpholino (MO). Control larvae received standard control MO. **(B)** Macrophages were depleted via clodronate liposome i.v. injection at 1 dpf. Control larvae received PBS liposomes. **(C)** Neutrophil-defective larvae (*mpx:rac2D57N*) were compared to wild-type larvae. Data are pooled from three independent replicates and the total larval N per condition is indicated in each figure. Cox proportional hazard regression analysis was used to calculate P values and hazard ratios (HR). Average injection CFUs: (A) control MO = 25, *pu.1* MO = 24, (B) PBS liposomes = 20, clodronate liposomes = 23, (C) wild-type = 26, *mpx:rac2D57N* = 22.

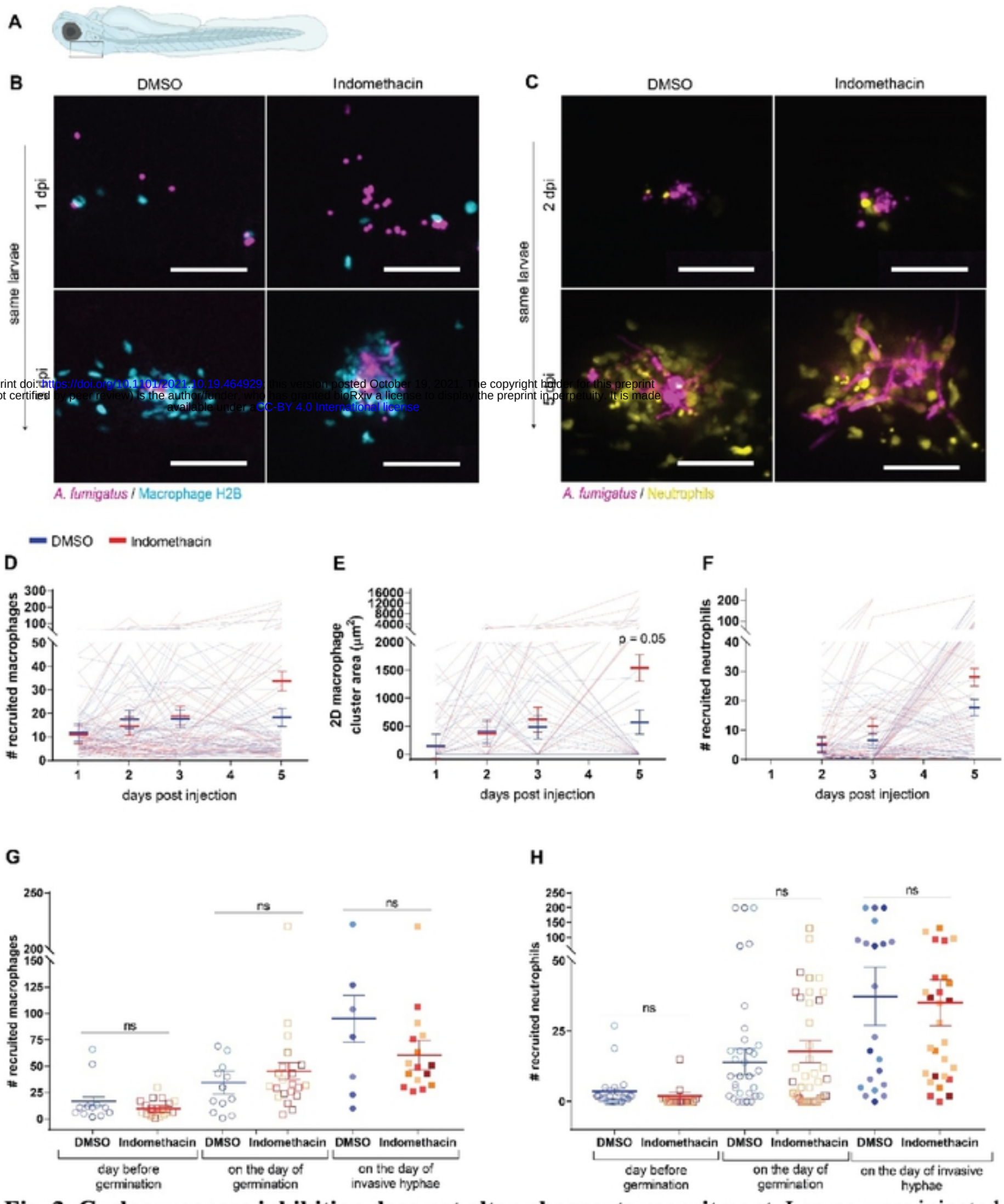

Fig. 3. Cyclooxygenase inhibition does not alter phagocyte recruitment. Larvae were injected with mCherry-expressing *A. fumigatus* TBK5.1 (Af293) spores at 2 dpf. After injection larvae were exposed to 10 μM indomethacin or DMSO vehicle control and were imaged through 5 dpi.

(A) Schematic showing the infection and imaging area of zebrafish larvae. **(B, D, E, G)** Macrophage nuclear-labeled *Tg(mpeg1:H2B-GFP)* larvae were imaged at 1, 2, 3, and 5 dpi. **(C, F, H)** Neutrophil-labeled *Tg(lyz:BFP)* larvae were imaged at 2, 3, and 5 dpi. (B, C) Representative z-projection images showing macrophage and neutrophil recruitment. Scale bars = 50 μm. (D) Number of macrophages recruited, (E) 2D macrophage cluster area, and (F) number of neutrophils recruited were quantified. Each line represents an individual larva followed for the entire course of infection and bars represent pooled emmeans ± SEM from four independent replicates, at least 12 larvae per condition, per replicate. P values were calculated by ANOVA. (G) Number of macrophages and (H) neutrophils one day before germination occurred, on the day of germination, and on the day invasive hyphae occurred were quantified. Bars represent pooled emmeans ± SEM from all larvae with germination from four independent replicates. Data points represent individual larva and are color coded by replicate. P values were calculated by ANOVA.

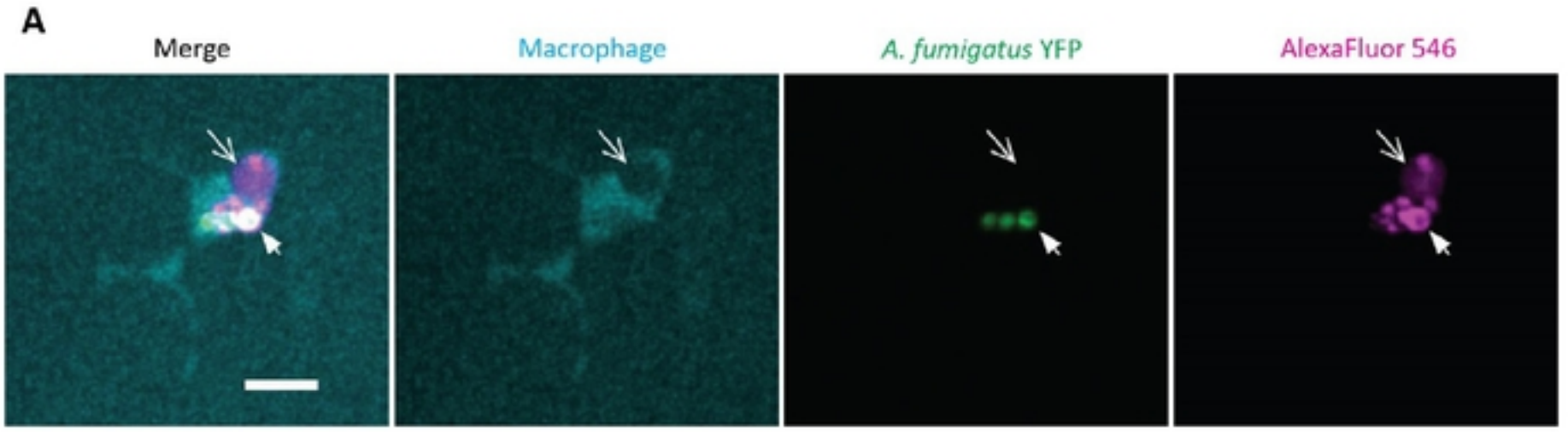

Fig. 4. Cyclooxygenase inhibition does not affect spore killing. (A, B) Macrophage-labeled larvae *Tg(mfap4:mTurquoise2)* were injected with YFP-expressing *A. fumigatus* TBK1.1 (Af293) spores coated with AlexaFluor 546 at 2 dpf, exposed to 10 μM indomethacin or DMSO vehicle control, and imaged at 2 dpi. (A) Representative images showing live (white arrow) and dead (open arrow) spores within a macrophage. Scale bar = 10 μm. Z projection of three slices. (B) The percentage of live spores in the hindbrain, and specifically within macrophages, per larvae. Each data point represents an individual larvae, color-coded by replicate (indomethacin n = 31, DMSO n = 30). Bars represent pooled emmeans ± SEM from three independent replicates, P values calculated by ANOVA. **(C)** Wild-type larvae were injected with TBK1.1 (Af293) spores at 2 dpf, exposed to 10 μM indomethacin or DMSO vehicle control, and fungal burden was quantified by homogenizing and plating individual larvae for CFUs at multiple days post injection. Eight larvae per condition, per dpi, per replicate were quantified, and the number of

CFUs at each dpi is represented as a percentage of the initial spore burden. Bars represent pooled emmeans ± SEM from three individual replicates, P values calculated by ANOVA. Average injection CFUs: 27.

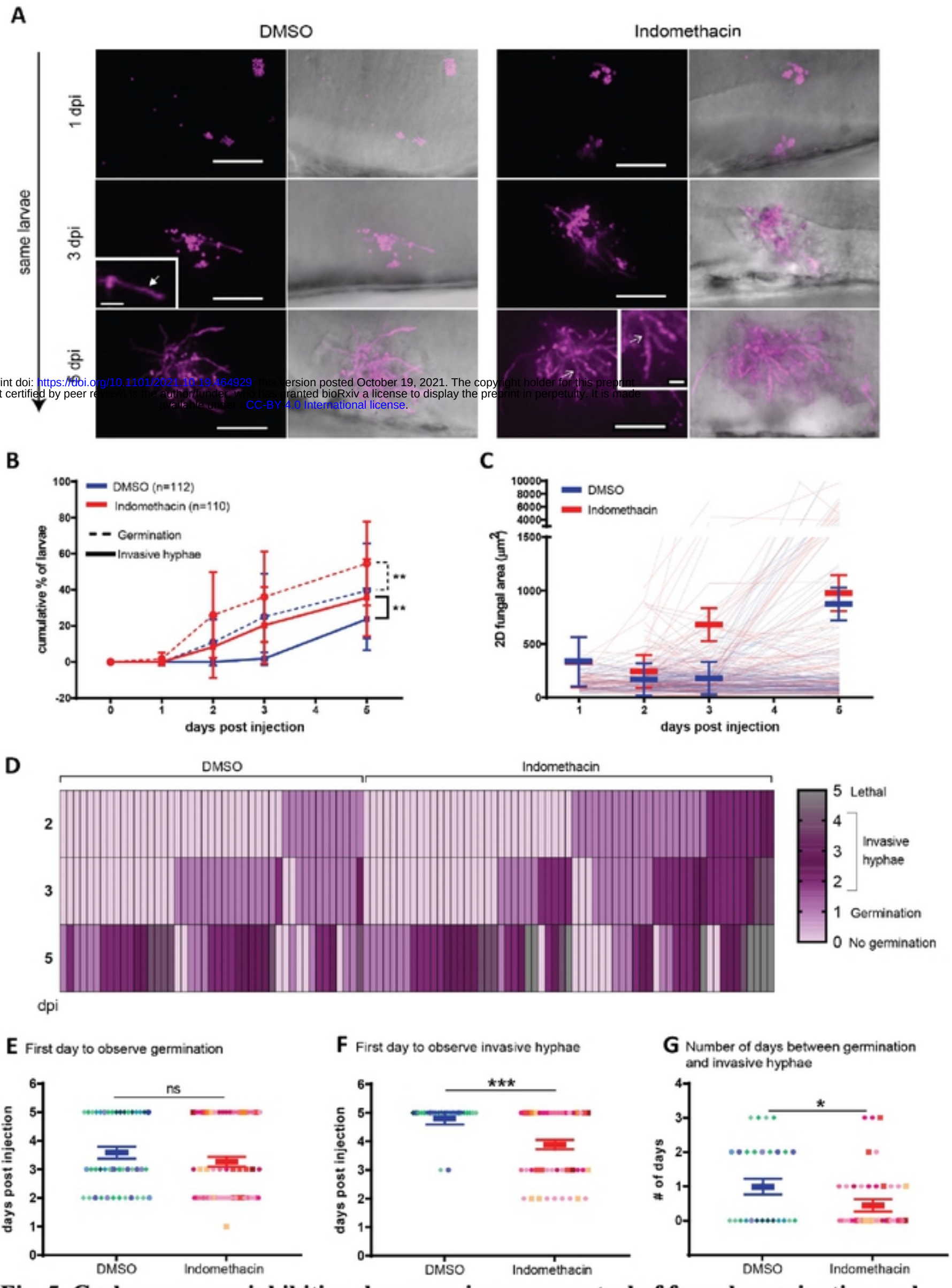

Fig. 5. Cyclooxygenase inhibition decreases immune control of fungal germination and

invasive hyphal growth. Zebrafish larvae were injected with mCherry-expressing TBK5.1 (Af293) spores at 2 dpf, exposed to 10 μM indomethacin or DMSO vehicle control and imaged at 1, 2, 3, and 5 dpi. **(A)** Representative images showing spore germination (inset white arrow) and invasive hyphae (branched hyphae, inset open white arrow). Scale bar = 50 μm (10 μm in insets). **(B)** Cumulative percentage of larvae with germination (dotted line) and invasive hyphae (solid line) through 5 dpi. Cox proportional hazard regression analysis was used to calculate P values. **(C)** 2D fungal area was quantified from image z projections. Each line represents an individual larva and bars represent pooled emmeans ± SEM from 8 independent replicates, at least 12 larvae per condition, per replicate. **(D)** Severity of fungal growth was scored for all larvae and displayed as a heatmap. Representative images for each score can be found in S5 Fig. **(E-G)** In larvae in which (E) germination (indomethacin n = 61, DMSO n = 45) and (F) invasive hyphae occurred (indomethacin n = 42, DMSO n = 27), the day on which each was first observed is plotted. (G) The number of days between germination and invasive hyphae was also calculated. Bars represent pooled emmeans ± SEM from eight individual replicates, P values calculated by ANOVA. Each data point represents an individual larvae, color-coded by replicate.

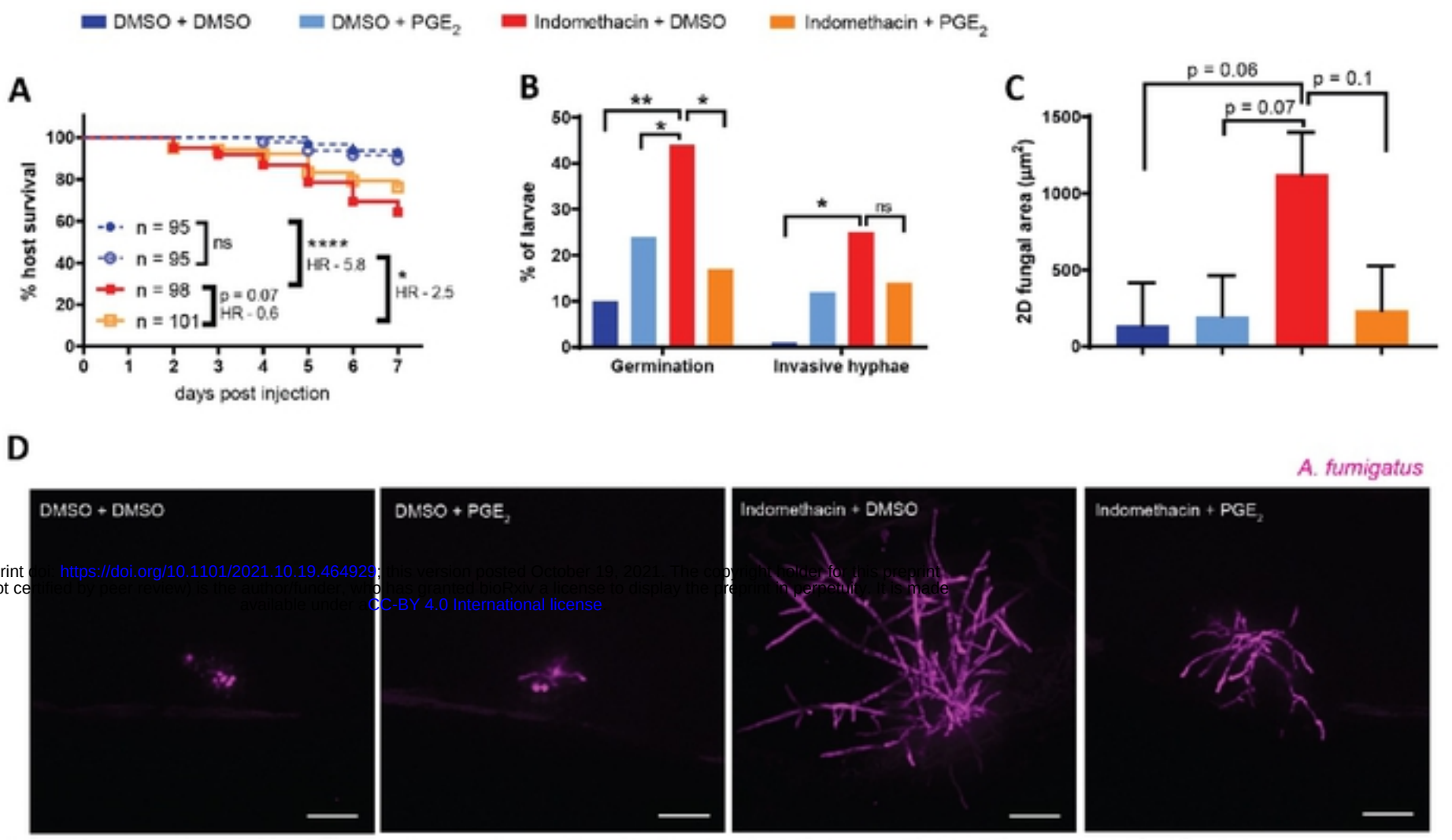

Fig. 6. Exogenous PGE_2 can rescue the indomethacin-mediated increase in fungal germination and hyphal growth. Larvae were injected with mCherry-expressing TBK5.1 (Af293) spores and exposed to 10 μM indomethacin or DMSO vehicle control at 2 dpf. At 1 dpi, larvae were injected with 10 μM PGE_2 or DMSO vehicle control. **(A)** Survival of wild-type larvae was monitored. Cox proportional hazard regression analysis was used to calculate P values and hazard ratios (HR). Data are pooled from four independent replicates, and total larval N per condition is indicated in figure. Average injection CFUs: 40. **(B-D)** Larvae were imaged at 3 dpi. (B) Percentage of larvae with germination and invasive hyphae, and (C) 2D fungal area in each condition. Data pooled from three independent replicates, at least 8 larvae per condition, per replicate, P values calculated by ANOVA. (C) Bars represent pooled emmeans ± SEM. (D) Representative images showing hyphal growth in each condition. Scale bars = 50 μm.

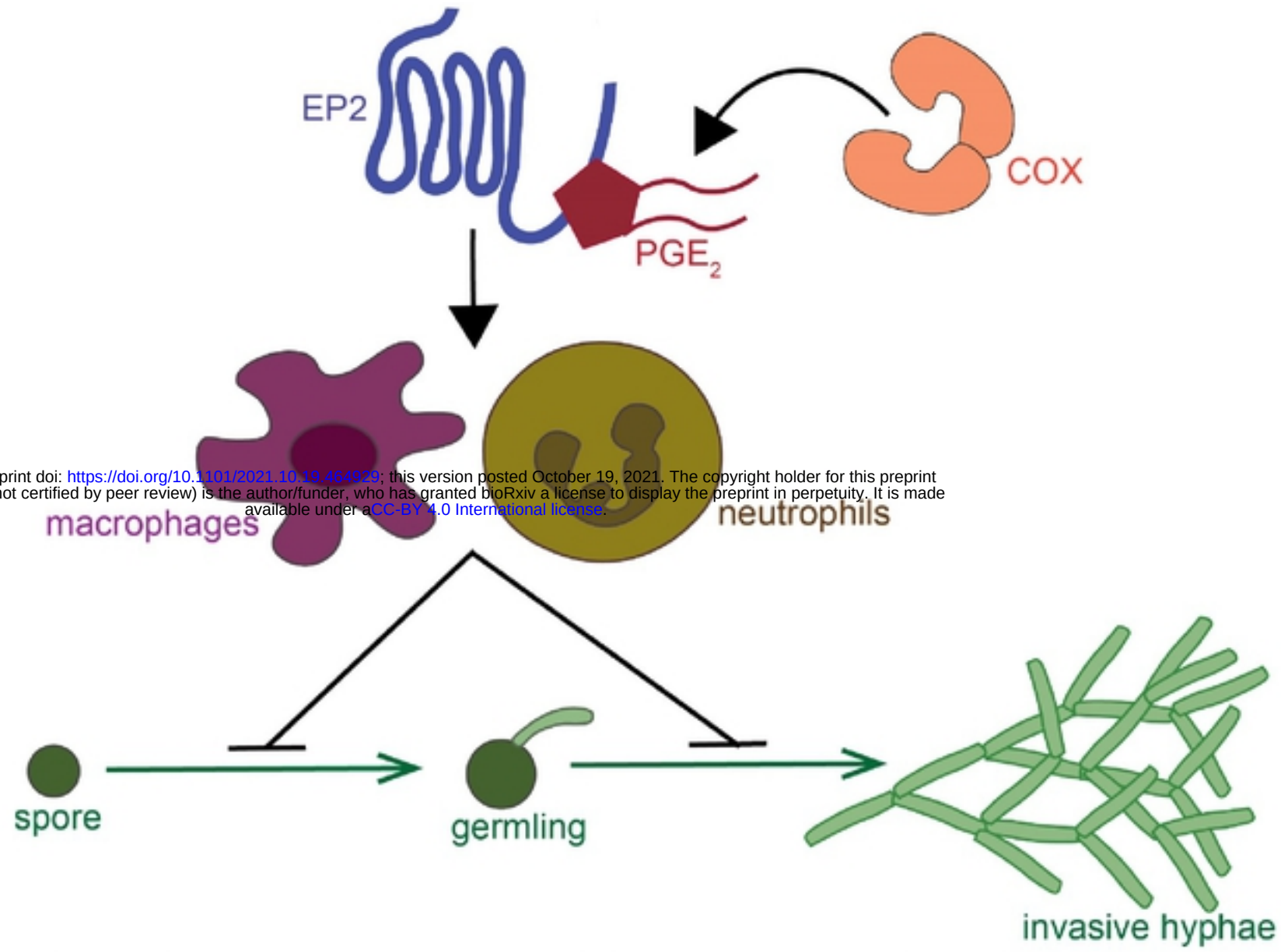

Fig. 7. Model of cyclooxygenase signaling in response to *A. fumigatus* growth. COX enzymes produce prostaglandin signaling molecule, including PGE_2. PGE_2 can bind to the EP2 receptor to exert pro-inflammatory effects. Zebrafish larvae injected with *A. fumigatus*, this signaling activates both macrophages and neutrophils to inhibit spore germination and development of invasive hyphal growth.